Band calculations for 4f systems based on the dynamical mean field theory

2007 J. Phys.: Condens. Matter 19 365213

(http://iopscience.iop.org/0953-8984/19/36/365213)

IOP PUBLISHING JOURNAL OF PHYSICS: CONDENSED MATTER

J. Phys.: Condens. Matter **19** (2007) 365213 (8pp) doi:10.1088/0953-8984/19/36/365213

Band calculations for 4f systems based on the dynamical mean field theory

Osamu Sakai[1] **and Yukihiro Shimizu**[1,2]

[1] Department of Physics, Tokyo Metropolitan University, Hachioji 192-0397, Japan
[2] Department of Applied Physics, Tohoku University, Sendai 980-8579, Japan

E-mail: sakai@phys.metro-u.ac.jp

Received 2 December 2006, in final form 27 February 2007
Published 24 August 2007
Online at stacks.iop.org/JPhysCM/19/365213

Abstract

Recent band calculations for Ce compounds based on the dynamical mean field theory (DMFT) are reported. The auxiliary impurity problem has been solved by a method named NCAf^{2}vc, which includes the correct exchange process of the $f^1 \rightarrow f^0, f^2$ virtual excitation, the crystalline field splitting (CFS), and the spin–orbit interaction (SOI) of the self-energy. These are necessary features in the quantitative band theory for Ce compounds. The results of applications on Ce metal and Ce-monopnictides are presented.

1. Introduction

The non-empirical band calculation for strongly correlated electron systems has been extensively developed on the basis of the dynamical mean field theory (DMFT) [1]. The 4f electrons in Ce compounds are typical strongly correlated electrons [2]. The 4f state splits into the $j = 5/2$ ground multiplet and the $j = 7/2$ excited multiplet with a separation of about 0.3 eV by the spin–orbit interaction (SOI). The multiplet shows crystalline field splitting (CFS) of the order of 100 K. In cubic crystals, the $j = 5/2$ multiplet splits into the $(j = 5/2)\Gamma_7$ doublet and the $(j = 5/2)\Gamma_8$ quartet. Hereafter, we call them Γ_7 and Γ_8 states, respectively. It is important to take account of the SOI and the CFS in 4f systems [2]. In the DMFT, the correlated band electron problem is mapped onto the calculation of the single particle excitation spectrum of the auxiliary impurity Anderson model in an effective medium. Reliable methods to solve the impurity problem with CFS and SOI are needed in the DMFT band calculation for 4f compounds.

A theory, which is named NCAf^{2}vc, has been developed [3, 4] and combined with the linear muffin tin orbital (LMTO) method to carry out the DMFT band calculation [5–7]. NCAf^{2}vc can include the CFS and SOI effects, and also the correct exchange process of the $f^1 \rightarrow f^0, f^2$ valence fluctuation. The calculation gives the accurate order of the Kondo temperature. We report results of the DMFT band calculation for Ce metal and Ce-monopnictides.

Ce metal is known to have iso-structural fcc phases [8]. The low temperature state is called the α phase and it has a smaller lattice constant. The higher temperature state is called the γ phase. DMFT studies on this transition have been extensively carried out [1][3]. In these studies the SOI and the CFS were neglected. In the present study we are not concerned with the α–γ transition, but we calculate the photo-emission spectra (PES) [9, 10] (see footnote 3) for the fcc state with the lattice constant of these two cases. The hybridization intensity (HI) estimated by the local density approximation (LDA) band has a peak near the Fermi energy (E_F). This peak is reduced in the DMFT band, thus the SOI side peak in PES becomes relatively conspicuous. The Kondo temperature (T_K) in the lower CFS state with Γ_7 is estimated to be around 25 K, and the excitation energy from Γ_7 to Γ_8 to be 90 K by calculation of the magnetic excitation in γ-Ce. In α-Ce, T_K becomes very high, about 2000 K.

Ce pnictides (CeBi, CeSb, CeAs, CeP, and CeN) show various anomalous properties such as the ferromagnetic double layer structure in the anti-ferromagnetic ordered state [11–13][4]. The compounds have semimetal band structure with a very small number of carriers [14]. The top of the valence bands has the Γ_8 character and has very strong mixing matrix elements with the Γ_8 components of 4f electrons, but the density of states (DOS) of the bands at E_F is small, reflecting the semimetal nature of the bands. The symmetry selective p–f mixing between holes and the 4f states plays an important role in the p–f mixing model, which was proposed by Kasuya *et al* [13, 14] to explain the anomalous magnetic properties in these compounds.

Intensive studies on PES of Ce pnictides have been carried out [9]. They have a characteristic double peak structure: a shallow-energy peak (SP) has a binding energy of about 0.8–0.4 eV and a deep-energy peak has a binding energy of about 3 eV. The SP is ascribed to the p–f bonding state of the hole excitation [15, 16]. The intensity of SP increases gradually as the pnictogen changes from Bi to P, and CeN is expected to show α-Ce like properties [9]. The DMFT band calculation has already been tried for Ce pnictides, but the CFS and SOI have not been included in the calculation [17]. A systematic application of the method for a series of Ce pnictides is needed.

In section 2, the calculation method is briefly explained. In section 3, we present results for Ce metal. An overview of applications to Ce pnictides is shown in section 4, and a summary is given in section 5.

2. Calculation method

Since the methods have been already described in [5] and [7], we exclude the detailed explanation from this paper. First of all we calculate self-consistent LDA bands based on the LMTO method, and potential parameters except for the f levels are fixed to those of the LDA calculation.

The DMFT band calculation is carried out in the following way. (I) We calculate the local self-energy of the auxiliary impurity Anderson model with a trial HI and 4f levels by the NCAf^{2}vc method. (II) Bloch states are calculated without the self-energy term for the LDA band parameters. (III) Next the matrix elements of the local self-energy for 4f states between Bloch states are calculated. (IV) Then the Greenian for the DMFT bands is calculated in this manifold of space, and the DOS of DMFT bands for a given wavenumber vector is calculated. (V) The local DOS is obtained by summing up over the wavenumber vectors. The calculation is repeated iteratively so that DOSs of the local auxiliary impurity model and the DMFT bands satisfy self-consistent conditions.

[3] See for example, references in [5].
[4] See for example, references in [7].

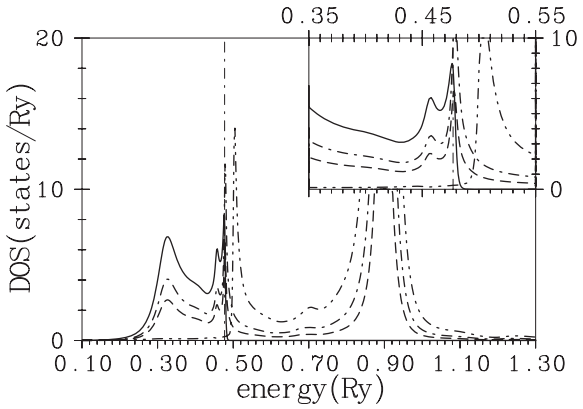

Figure 1. The 4f DOS of γ-Ce at $T = 300$ K. The solid line is the total 4f PES. The dashed line is the DOS of the ($j = 5/2$) Γ_7 component, the dot–dashed line is DOS of the ($j = 5/2$) Γ_8 component, and the two-dots–dashed line is DOS of the $j = 7/2$ component. The Fermi energy E_F is indicated by the vertical dot–dashed line. The inset shows spectra near the Fermi energy. $a = 9.754\,77$ AU and n_f(rsl.target) $= 0.982$.

The 4f level position is adjusted in the DMFT self-consistent loops so that the 4f occupation number has a given target value, which is estimated from the LDA band calculation. The target 4f electron number n_f(rsl.target) is imposed on the occupation number calculated directly by the resolvents in order to stabilize the self-consistency iteration loop. The occupation number obtained by the integration of the 4f DOS, n_f(intg.), has deviation within 0.5% of that calculated directly by the resolvents because many intermediate calculations are contained.

3. Ce metal

In figure 1, we show the 4f DOS of γ-Ce at $T = 300$ K obtained by the present DMFT calculation. The target occupation number is set to be n_f(rsl.target) $= 0.982$, which has been used in previous calculations [5, 7]. The occupation number of the $j = 7/2$ component, 0.03, is very small. The mass enhancement factor of this component is small compared with that of $j = 5/2$ components. (See for example, the caption of figure 4.) The effective level $\bar{\varepsilon}_\Gamma$ for $j = 7/2$ is located far above E_F. The $j = 7/2$ component is almost silent for states very near E_F in γ-Ce.

The 4f DOS obtained by using the HI of LDA is shown in figure 2. In the LDA calculation, the SOI side peak merges into the stronger Kondo resonance peak at E_F. The SOI side peak becomes conspicuous in the DMFT calculation because the HI near E_F is reduced. This reduction is caused mainly by the reduction of 4f DOS from the Fermi energy region (i.e. the main spectral intensity of 4f bands shift up to the energy region of f^2 states).

The HI is reduced in DMFT, but the calculated DOS still has a shape of more f^0-like character systems, when it is compared with experimental results: relatively stronger intensity of the Kondo peak compared with that of the SOI side peak [9, 10]. From the calculation of the magnetic excitation spectrum, T_K in the Γ_7 is estimated to be about 25 K, and the $\Gamma_7 \rightarrow \Gamma_8$ excitation energy about 90 K, though they are not so separated [18]. When we choose a larger number for n_f(rsl.target), the intensity of the Kondo resonance peak decreases and the SOI side peak becomes relatively large, while the binding energy of the deep peak becomes too large. For example, the case of n_f(rsl.target) $= 1.008$ leads to the binding energy 3.1 eV.

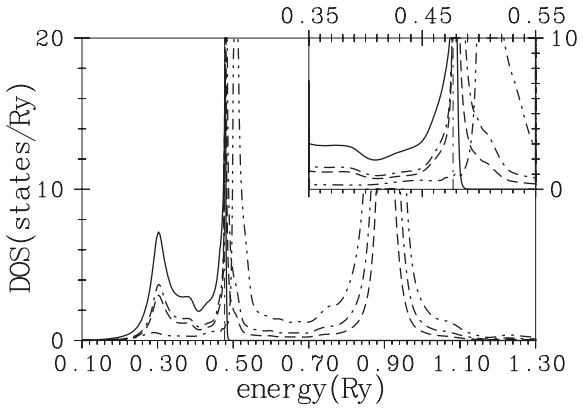

Figure 2. The 4f DOS of γ-Ce at $T = 300$ K calculated by using the hybridization intensity of the LDA band. For definitions of the lines, see the caption of figure 1.

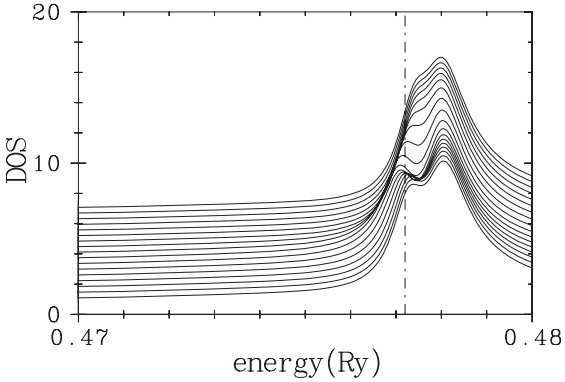

Figure 3. The $\boldsymbol{k}$-dependent 4f DOS of γ-Ce at $T = 53$ K. The wavenumber vector $\boldsymbol{k}$ is changed from the Γ point (bottom) to the L point (top) along the Λ line in the Brillouin zone. The levels of lines are shifted by 0.375.

We note, the NCAf^{2}vc method gives rather higher T_K when compared with the result of numerical renormalization group (NRG) calculations which will give a more correct T_K value [7]. The origin of the discrepancy may be partly ascribed to this point, and partly to the neglect of interaction effects beyond the LDA for the usual band components, i.e. for the 5d band part. At the present stage, however, we may say that the DMFT calculation gives a rather good quantitative result when we consider the fact that the Kondo temperature quite drastically depends on the hybridization strength.

In figure 3, we show f-DOS at $T = 53$ K when the wavenumber vector runs from the Γ (Gm) to the L point along the Λ (Lm) line. The renormalized band (RNB) dispersion is shown in figure 4. The energy shift (the real part of the self-energy) at E_F and the renormalization factor (mass enhancement factor) are taken into account in this calculation. Very flat bands with the $j = 5/2$ character appear just above E_F because the mass enhancement factor is large. Flat bands for $j = 7/2$ appear around the energy 0.55 Ryd in RNB, but peaks corresponding to the $j = 7/2$ components are located at about 0.50 Ryd in the f-DOS. The RNB picture has only a limited meaning, because the imaginary part and the energy dependence of the real part is not small in the present calculation. However, we can see some corresponding

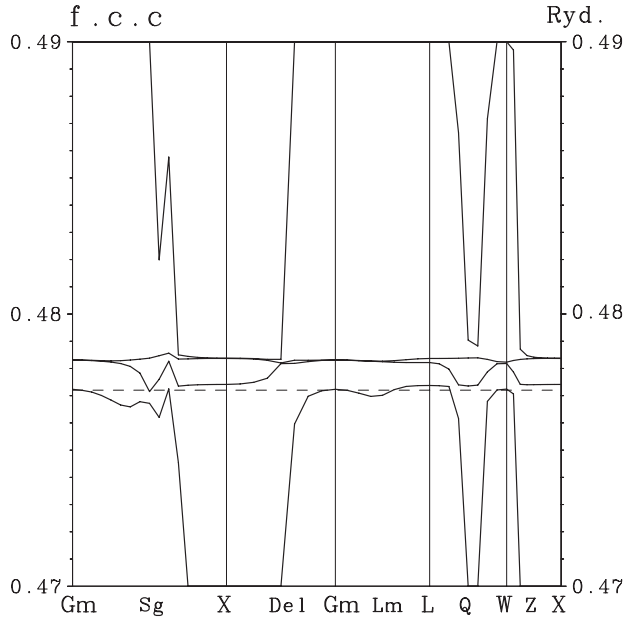

Figure 4. Renormalized band (RNB) structures of γ-Ce at $T = 53$ K. The Fermi energy E_F is indicated by the dashed line. The self-energy shift and its derivative at E_F are taken into account. The imaginary part is set to be zero. The effective levels measured from E_F ($\bar{\varepsilon}_\Gamma$) and mass renormalization factor ($\bar{Z}_\Gamma^{-1}$) are: ($\bar{\varepsilon}_\Gamma$, $\bar{Z}_\Gamma^{-1}$) = (0.0135 Ryd, 50.3), (0.0681 Ryd, 55.5) and (0.2892 Ryd, 3.6) for Γ_7, Γ_8 and $j = 7/2$ components, respectively.

features near E_F between figures 3 and 4. In the RNB of figure 4, a band cuts E_F on the Λ (Lm) line. This feature is also seen in figure 3. We will have a hole-like Fermi surface around the Γ point at very low temperatures. A similar hole-like surface is expected in the LDA band calculation of γ-Ce. The 'Fermi surface' structure of the present RNB dispersion is qualitatively similar to that of the LDA calculation. Of course, the dispersion is very small in the DMFT calculation for bands with 4f character.

When we calculate the RNB dispersion at $T = 300$ K, the 4f bands are located at higher energy because the mass enhancement factor is not so large. The band which cuts E_F on the Λ line in figure 4 rises up above E_F. The 'Fermi surface' structure of the RNB at $T = 300$ K is similar to that of the La metal. The same behaviour has already been noted for CeSb in [7]. The 4f DOS becomes almost dispersionless on the Λ line because the very fine structures of the 4f DOS are smeared out at $T = 300$ K.

In figure 5 we show the 4f-DOS of α-Ce. In experiments, the binding energy of the deep f level is almost equal to that of γ-Ce [9], but this fact has not been reproduced in the present calculation. The deep f is usually located below the bottom of the conduction band because the band repelling is very large due to strong HI in α-Ce. The binding energy decreases only slowly when the target number n_f(rsl.target) is decreased drastically. It is tentatively chosen to be 0.91. T_K is estimated to be about 2000 K from the magnetic excitation.

4. Ce pnictides

Ce pnictides have the NaCl structure in which Ce ions form the fcc lattice (see footnote 4). The valence and the conduction bands mainly consist of the pnictogen p states and the Ce 5d states,

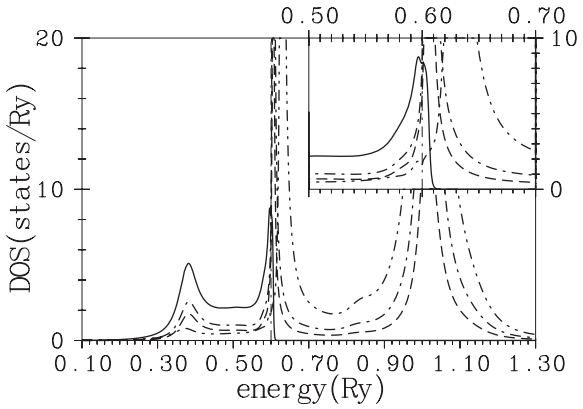

Figure 5. The 4f DOS of α-Ce at $T = 10^3$ K. The target value n_f(rsl.target) is set to be 0.982. For definitions of the lines, see the caption of figure 1. $a = 9.165\,17$ AU.

respectively. They overlap slightly and form semi-metallic band structures (see footnote 4). The top of the p valence band has the $(j = 3/2)\Gamma_8$ character, and thus has a strong hybridization matrix with the 4f states of the Γ_8 character.

The symmetry selective p–f mixing between holes and the 4f states plays an important role in the p–f mixing model. A part of the Γ_8 valence band which has the same symmetry as the occupied 4f band is pushed up above E_F due to the hybridization [14]. The re-construction of the electronic band structures in the ordered states is expected by the Hartree–Fock-like static mean field theory [20], and confirmed by experimental studies [21] (see footnote 4). We need the DMFT band calculation in the paramagnetic phase.

In figure 6, we show 4f-DOS for a series of Ce pnictides calculated at $T = 300$ K. The d–p band overlapping of the simple LDA calculation is large compared with the experimental result, as noted in previous papers [20]. We tentatively shift the p valence band to the low energy side by 0.8 eV in the calculation. The atomic energy level of Γ_7 is additionally shifted. This extra shift of Γ_7 is denoted as ΔE_7, and may correspond to the CFS due to the electrostatic potential. It has almost no effect in the usual LDA band calculation, but a large effect on the relative occupancy of Γ_7 and Γ_8 in the DMFT calculation. We have chosen ΔE_7 somewhat arbitrarily so that the relative occupation of Γ_7 becomes larger than that of Γ_8 at $T = 300$ K, as expected in experiments (see footnote 4).

Calculations for all compounds except CeN show good correspondence with the experimental results of the double peak structure in PES [9]: the deep peak appears at a binding energy of about 3 eV and the SP appears around 0.5 eV; the intensity of the SP increases as the pnictogen goes from Bi to P; the binding energy of the SP decreases from 0.7 eV for CeSb to 0.3 eV for CeP. Except for the case of CeN, the occupation number of the $j = 7/2$ component is very small.

At 300 K, the DOS of the f component is small on E_F. The effective HI has a dip near E_F with several fine structures. In low temperature cases, we have states with finite 4f DOS at E_F and $T_K \sim 50$ K for CeSb. In such cases, the HI has broad peaks near E_F.

In the CeN case, a very strong 4f peak appears just above E_F, reflecting the strong HI in this compound in the calculation at $T = 10^3$ K, even when n_f(rsl.target) is set to be 1.008. A dip appears at E_F in the 4f DOS at $T = 300$ K. It may be an artificial result from the NCA method because T_K, which is estimated by calculation of the magnetic excitations, is about 0.3 eV. The NCA method fails at very low temperatures compared with T_K [19].

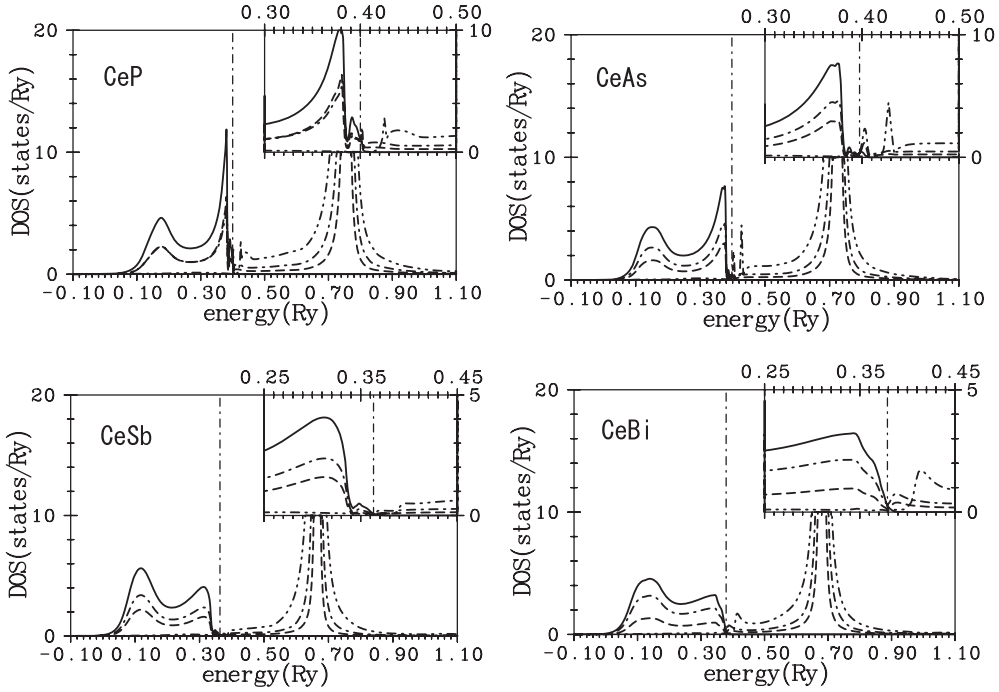

Figure 6. The 4f DOS of Ce pnictides at $T = 300$ K. The target value n_f(rsl.target) is commonly set to be 1.008, and the point charge part of CFS for CeBi is taken ($\Delta E_7 = -230$ K) into account as follows: CeBi ($\Delta E_7 = -230$ K), CeSb ($\Delta E_7 = -250$ K), CeAs ($\Delta E_7 = -300$ K), CeP ($\Delta E_7 = -350$ K). For definitions of the lines, see the caption of figure 1.

5. Summary and discussion

In this paper, we have reported the results of the DMFT band calculation for Ce metal and Ce pnictides. The auxiliary impurity problem is solved by a method named NCAf^{2}vc, which includes the correct exchange process of the $f^1 \rightarrow f^0$ and $f^1 \rightarrow f^2$ virtual excitation. The splitting of the self-energy due to the spin–orbit interaction (SOI) and the crystalline field splitting (CFS) effect is considered. The DMFT band calculation adopting the NCAf^{2}vc method reproduces semi-quantitatively the systematics of the PES of these compounds, but some discrepancies remained.

In γ-Ce, the SOI side peak appears in the DMFT calculation because HI is reduced near E_F in the DMFT calculation. It merges with the Kondo resonance peak at E_F when we directly use HI of the LDA band. However, the present calculation still gives stronger HI than that expected from PES experiments. The HI in α-Ce seems also to be too strong. The dispersion of the 4f bands is expected, and it leads to a Fermi surface structure similar to that of the LDA band at low temperatures.

The systematics of the PES of Ce-pnictides, such as the double peak structure, show good correspondence with experimental results. Through the application of the present DMFT-NCAf^{2}vc band calculation scheme to Ce compounds, its effectiveness and weaknesses are recognized. Calculations of the 4f band state in various Ce compounds will be carried out in the near future.

Acknowledgments

The authors would like to thank H Shiba, J Flouquet, T Fujiwara, S Tsuneyuki, T Saso, Y Kuramoto, H Harima, and J Otsuki for stimulating discussions. The numerical computation was partly performed in the Computer Center of Tohoku University and the Supercomputer Center of the Institute for Solid State Physics (University of Tokyo). This work was partly supported by Grant-in-Aid for Scientific Research Nos 17064004 and 18027004.

References

[1] Held K, Nekrasov I A, Keller G, Eyert V, Blümer N, McMahan A K, Scalettar R T, Pruschke T, Anisimov V I and Vollhardt D 2002 *Proc. Winter School on Quantum Simulations of Complex Many-Body Systems: From Theory to Algorithms (Rolduc/Kerkrade (NL), Feb.–March 2002)*
Held K, Nekrasov I A, Keller G, Eyert V, Blümer N, McMahan A K, Scalettar R T, Pruschke T, Anisimov V I and Vollhardt D 2001 *Preprint* cond-mat/0112079
[2] Allen J W 2005 *J. Phys. Soc. Japan* **74** 34
[3] Sakai O, Motizuki M and Kasuya T 1988 *Core-Level Spectroscopy in Condensed Systems Theory* ed J Kanamori and A Kotani (Berlin: Springer) p 45
[4] Otsuki J and Kuramoto Y 2006 *J. Phys. Soc. Japan* **75** 064707
[5] Sakai O, Shimizu Y and Kaneta Y 2005 *J. Phys. Soc. Japan* **74** 2517
[6] Sakai O and Shimizu Y 2007 *J. Magn. Magn. Mater.* **310** 374 (a part of the present work has been reported in the *ICM 2006 (Kyoto, Aug. 2006)*)
[7] Sakai O and Shimizu Y 2007 *J. Phys. Soc. Japan* submitted
[8] Koskenmaki D G and Gschneidner K A Jr 1978 *Handbook on the Physics and Chemistry of Rare Earths* ed K A Gschneidner Jr and L Eyring (Amsterdam: North-Holland) p 337
[9] Baer Y and Schneider W-D 1987 *Handbook on Physics and Chemistry of Rare-Earths* vol 10, ed K Gschneidner, L Eyring and S Hüfner (Amsterdam: North-Holland) p 1
Lynch D W and Weaver H 1987 *Handbook on Physics and Chemistry of Rare-Earths* vol 10, ed K Gschneidner, L Eyring and S Hüfner (Amsterdam: North-Holland) p 231
Hillebrecht F U and Campagna M 1987 *Handbook on Physics and Chemistry of Rare-Earths* vol 10, ed K Gschneidner, L Eyring and S Hüfner (Amsterdam: North-Holland) p 425
[10] Higashiguchi M, Shimada K, Narimura T, Namatame H and Taniguchi M 2004 *Physica* B **351** 256
[11] Rossat-Mignod J, Burlet P, Quezel S, Effantin J M, Delacte D, Bartholin H, Vogt O and Ravot D 1985 *J. Magn. Magn. Mater.* **31–34** 398
[12] Hannan A, Iwasa K, Kohgi M and Suzuki T 2000 *J. Phys. Soc. Japan* **69** 2358
[13] Kasuya K, Takegahara K, Aoki Y, Suzuki T, Kunii S, Sera M, Sato N, Fujita T, Goto T, Tamaki A and Komatsubara T 1982 *Valence Instabilities* ed P Wachter and H Boppart (Amsterdam: North-Holland) p 359
[14] Takahashi H and Kasuya T 1985 *J. Phys. C: Solid State Phys.* **18** 2697
Takahashi H and Kasuya T 1985 *J. Phys. C: Solid State Phys.* **18** 2709
Takahashi H and Kasuya T 1985 *J. Phys. C: Solid State Phys.* **18** 2721
Takahashi H and Kasuya T 1985 *J. Phys. C: Solid State Phys.* **18** 2731
Takahashi H and Kasuya T 1985 *J. Phys. C: Solid State Phys.* **18** 2745
Takahashi H and Kasuya T 1985 *J. Phys. C: Solid State Phys.* **18** 2755
[15] Fujimori A 1983 *Phys. Rev.* B **27** 3992
[16] Takeshige M, Sakai O and Kasuya T 1985 *J. Magn. Magn. Mater.* **52** 363
[17] Lægsgaard J and Svane A 1998 *Phys. Rev.* B **58** 12817
[18] Holland-Moritz E and Lander G H 1994 *Handbook on Physics and Chemistry of Rare-Earths* vol 19, ed K Gschneidner, L Eyring, G H Lander and G R Choppin (Amsterdam: North-Holland) p 1
[19] Bickers N E 1987 *Rev. Mod. Phys.* **59** 845
[20] Kaneta Y, Iwata S, Kasuya T and Sakai O 2000 *J. Phys. Soc. Japan* **69** 2559
[21] Settai R, Goto T, Sakatsume S, Kwon Y S, Suzuki T, Kaneta Y and Sakai O 1994 *J. Phys. Soc. Japan* **63** 3026